FEATURES OF COSMIC-RAY DETECTION WITH A TWO-DETECTOR TELESCOPE

Krasimir Krastev[1], Jordanka Semkova[1], Rositza Koleva[1], Viktor Benghin[2], Sergey Drobyshev[2]

[1]Space Research and Technology Institute – Bulgarian Academy of Sciences
[2] Institute for Biomedical Problems – Russian Academy of Sciences
e-mail: bwfer@yandex.ru

Keywords: *cosmic rays; Geant4; Fe-56; secondary particles; coincidence detection.*

Abstract: *Cosmic-ray measurements with two-detector telescopes rely on coincident energy deposition in two sensitive volumes. Such coincidences, however, may arise from different physical mechanisms because interactions of primary particles with detector materials and surrounding structures generate secondary-particle cascades. This study examines complete particle histories for 1 GeV/nucleon Fe-56 nuclei simulated using a detailed Geant4 model of a two-detector silicon telescope. Three geometrical classes are investigated: Case 2, in which the primary intersects neither detector; Case 3, in which it intersects both detectors; and Case 5, in which it intersects only one detector. For each class, events with minimum and maximum total energy deposition in detector A are selected. Their particle trajectories, secondary species, genealogy, generation depth, and detector energy deposition are analyzed. Case 2 demonstrates coincidences generated exclusively by secondary particles, including electron-mediated signals and a high-deposition event involving an Fe-55 fragment. Case 3 provides the direct primary-traversal reference. Case 5 demonstrates mixed registration: the primary traverses detector A, while secondary electrons produce the signal in detector B. The selected Case 5 events additionally illustrate the strong influence of the primary path length within silicon, from partial edge traversal to passage along the detector width. These results show that identical coincidence criteria can select physically different events and that complete cascade reconstruction is essential for interpreting the response of cosmic-ray telescope detectors.*

ОСОБЕНОСТИ ПРИ РЕГИСТРАЦИЯТА НА КОСМИЧЕСКИ ЛЪЧИ С ДВУДЕТЕКТОРЕН ТЕЛЕСКОП

Красимир Кръстев[1], Йорданка Семкова[1], Росица Колева[1], Виктор Бенгин[2], Сергей Дробишев[2]

[1]Институт за космически изследвания и технологии – Българска академия на науките
[2]Институт по медико-биологични проблеми – Руска академия на науките
e-mail: bwfer@yandex.ru

Ключови думи: *космически лъчи; Geant4; Fe-56; вторични частици; регистрация на съвпадение*

Резюме: *Изследвани са механизмите на регистрация на космически лъчи в двудетекторен силициев телескоп чрез пълно проследяване на каскадите от частици, породени от ядра Fe-56 с енергия 1 GeV/нуклон. Анализирани са събития, при които първичната траектория не пресича нито един детектор (Case 2), пресича двата (Case 3) или само единия (Case 5). За всеки клас са разгледани събития с минимално и максимално енергоотделяне в детектор A. Определени са приносите на първичните и вторичните частици и влиянието на геометрията на преминаване върху регистрираната енергия.*

1. Introduction

Silicon telescope detectors identify charged-particle events by requiring energy deposition in two spatially separated sensitive volumes. Although this coincidence condition is useful for selecting penetrating radiation, the coincidence itself does not establish whether the original cosmic-ray particle crossed both detectors. Nuclear and electromagnetic interactions in the instrument and nearby structures can produce secondary particles that also deposit energy in the sensitive volumes.

This work continues the earlier Liulin-MO numerical study by Krastev [1], which established geometrical event classes and characterized secondary-induced coincidences statistically. Here the emphasis shifts to complete, event-by-event Fe-56 cascade histories.

2. Simulation model and event selection

The analysis uses Geant4 particle-transport outputs for Fe-56 primaries with kinetic energy 1 GeV per nucleon (56 GeV per nucleus), including a detailed representation of the silicon detectors and nearby instrument materials. The coincidence condition requires deposited energy exceeding 70 keV in both detectors A and B, independently of the identity of the depositing particles.

Geometrical classification is based on the primary trajectory, independently of subsequent interactions: Case 2 neither detector intersected; Case 3 both detectors intersected; Case 5 only detector A intersected. For each class, the event with the smallest and the event with the largest total energy deposition in detector A were selected. “MIN” and “MAX” therefore refer to detector-A energy deposition, not to the size of the cascade.

Complete step-level histories were examined to identify particle tracks, parent-daughter relationships, generation depth, interaction processes, and energy deposition in the sensitive volumes. The thick black line in trajectory visualizations marks the primary Fe-56 trajectory; colored lines denote secondary particles.

3. Results and discussion

3.1. Case 2: secondary-mediated coincidences

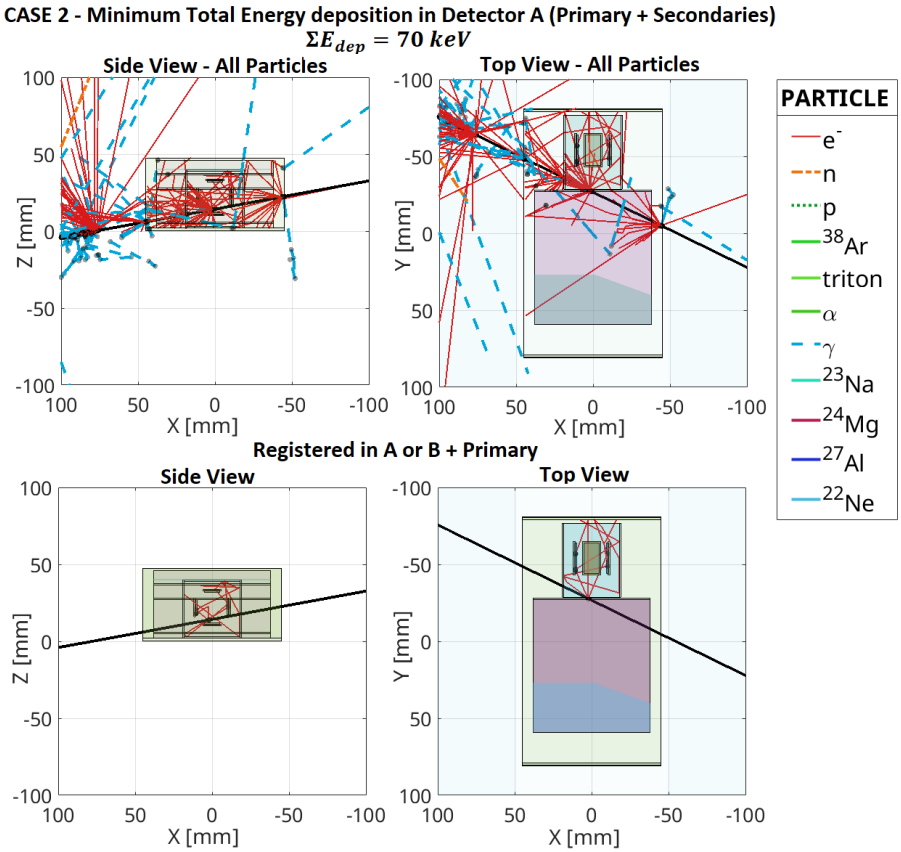


Fig. 1. Case 2 MIN: full cascade (top) and detector-contributing trajectories (bottom). Thick black line: primary Fe-56; colored lines: secondary particles.

Fig. 1 shows a Case 2 event in which the primary Fe-56 trajectory intersects neither detector. Nevertheless, secondary electrons deposit 0.07001 MeV in detector A and 0.92692 MeV in detector B, satisfying the coincidence condition. The cascade contains 2,466 tracks and 8,695 simulation steps and reaches generation five. Detector A receives its signal exclusively from secondary electrons. Two first-generation electrons originating in nearby textolite account for approximately 58.05 keV of the 70.01 keV signal; the remainder is supplied by further electron tracks. This event demonstrates a threshold-level coincidence without direct primary traversal.

The maximum-energy Case 2 event (Fig. 2) exhibits a markedly different mechanism. It contains 41,083 tracks and 94,623 steps, reaching generation nine. Detector A receives 469.278 MeV: 295.689 MeV (63.0%) from a secondary Fe-55 nucleus, 173.589 MeV (37.0%) from electrons, and a negligible photon contribution. Detector B receives 1.370 MeV from electrons. The Fe-55 fragment is a daughter of the primary Fe-56 nucleus. Thus, a large detector-A signal can be generated by a nuclear fragment even though the initial primary trajectory misses both sensitive volumes.

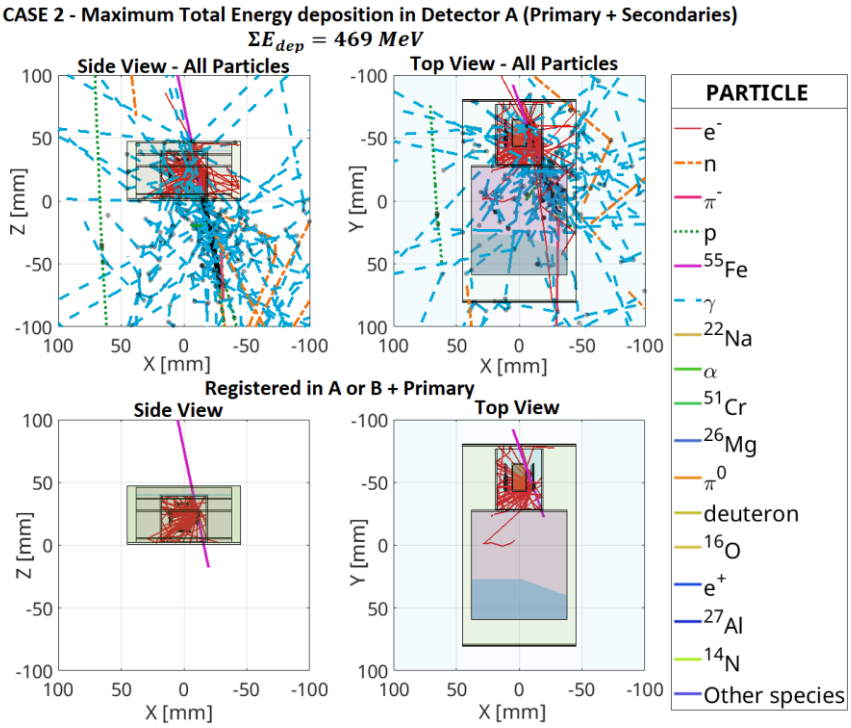


Fig. 2. Case 2 MAX: complete particle cascade and detector-contributing trajectories. The primary trajectory misses both detectors.

3.2. Case 3: genuine telescope traversals

Case 3 is the reference geometry for a genuine telescope traversal: the initial Fe-56 trajectory intersects both sensitive volumes. In the selected minimum-energy event (Event 90648350), the reconstructed history contains 12,692 tracks and 29,188 steps, with a maximum generation of four. The energy deposition is approximately 79.58 MeV in detector A and 78.71 MeV in detector B. The primary Fe-56 nucleus contributes approximately 51.25 and 50.81 MeV, respectively; secondary electrons account for most of the remaining energy.

For the selected maximum-energy Case 3 event (Event 60472254), 21,986 tracks and 51,175 steps are recorded, again with a maximum generation of four. The total energy deposition is approximately 117.22 MeV in detector A and 114.55 MeV in detector B. The primary deposits approximately 73.53 MeV in detector A and 73.55 MeV in detector B, with substantial additional electron contributions. These two events demonstrate direct heavy-ion traversal of both detectors, but also show that the measured energy is not necessarily attributable to the primary alone.

3.3. Case 5: mixed registration and path-length effects

Figures 3 and 4 illustrate the minimum-energy event selected for Case 5, in which the primary Fe-56 nucleus traverses detector A without intersecting detector B. Although the primary particle passes through only one of the two sensitive volumes, energy deposition is recorded in both detectors as a result of secondary-particle transport. This event therefore demonstrates how a two-detector coincidence can arise even when the primary ion does not directly cross both detectors.

The total simulated energy deposition in detector A is 11.164 MeV. Of this amount, 7.292 MeV (65.3%) is deposited directly by the primary Fe-56 nucleus, while secondary electrons contribute 3.873 MeV (34.7%). The contribution from photons is negligible. In detector B, the deposited energy is 0.789 MeV and is produced entirely by secondary electrons. Thus, the signal in detector B is not associated with a direct passage of the primary nucleus but with the transport of charged secondary particles generated during the development of the interaction cascade.

The enlarged three-dimensional view in Fig. 4 provides a clearer representation of the primary trajectory relative to the sensitive silicon volumes. In this particular event, the Fe-56 nucleus passes close to the boundary of detector A, resulting in a relatively short path through its active material. Consequently, the energy deposited directly by the primary particle is substantially lower than that expected for a trajectory crossing the full nominal detector thickness.

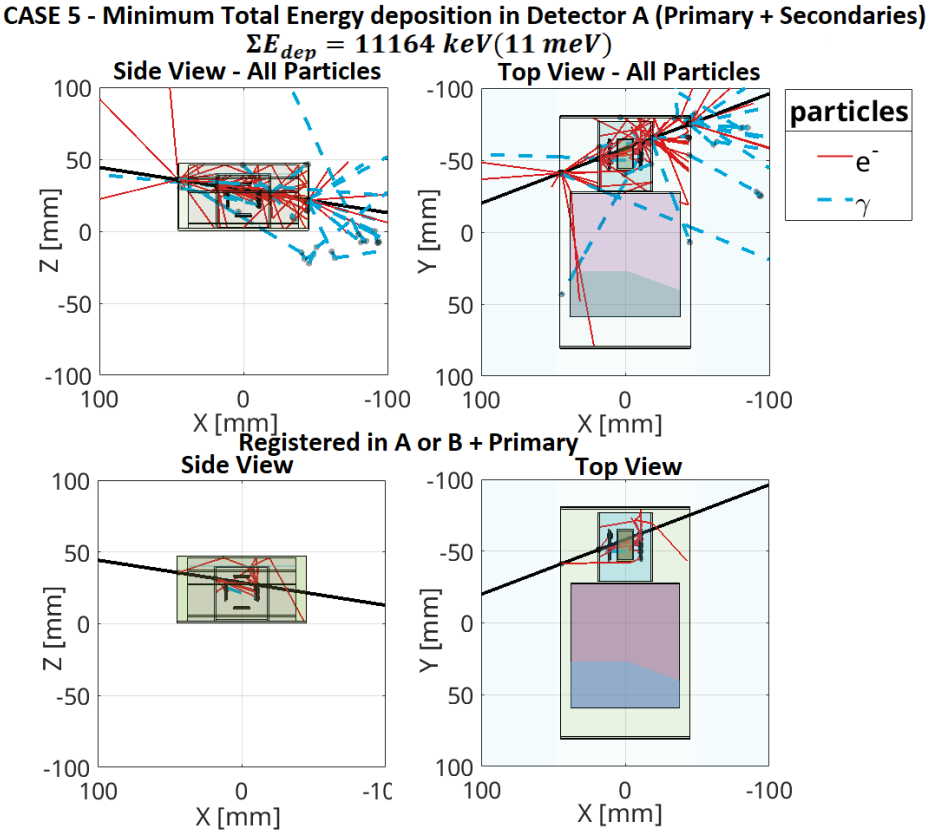


Fig. 3. Case 5 MIN: side and top projections of the full cascade and detector-contributing tracks. The thick black line shows primary Fe-56.

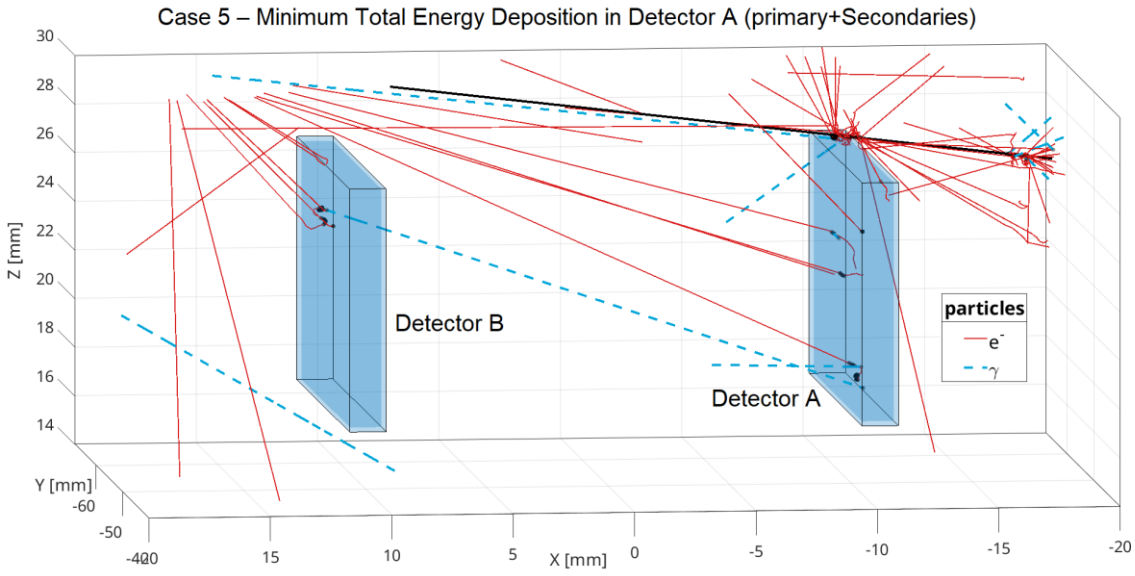


Fig. 4. Enlarged three-dimensional view of Fig. 3 showing only sensitive detectors A and B; red lines: electrons; dashed blue lines: photons.

For comparison, an Fe-56 ion with a kinetic energy of 1 GeV per nucleon traversing the nominal 300 µm silicon thickness would be expected to deposit approximately 80 MeV under the reference geometry considered in this study. The substantially smaller total energy deposition of 11.164 MeV in detector A is therefore consistent with a partial traversal of the sensitive volume. This comparison is qualitative, since the actual energy loss depends on the trajectory, effective path length, local interaction processes, and production and transport of secondary particles.

An important feature of this event is that secondary electrons account for approximately one-third of the total energy deposited in detector A, despite the relatively short primary-particle path. Their contribution illustrates that the recorded signal cannot always be interpreted solely in terms of the direct ionization losses of the incident heavy ion. Secondary-particle transport can modify the energy-deposition pattern in the detector traversed by the primary nucleus and simultaneously produce a detectable signal in the neighboring detector.

From the perspective of telescope response, the event highlights two distinct effects. First, trajectories passing near the boundaries of the sensitive volume may produce energy-deposition values substantially below those associated with a full-thickness traversal. Second, secondary particles may generate a signal in a detector that is not intersected by the primary ion. The combination of these effects can complicate the interpretation of coincidence events and contribute to the population of intermediate energy-deposition regions in simulated telescope spectra.

The present event should be regarded as an illustrative example rather than a statistically representative description of all Case 5 events. Nevertheless, it demonstrates the importance of considering the actual primary-particle trajectory together with the individual contributions of secondary particles when interpreting the response of a two-detector silicon telescope.

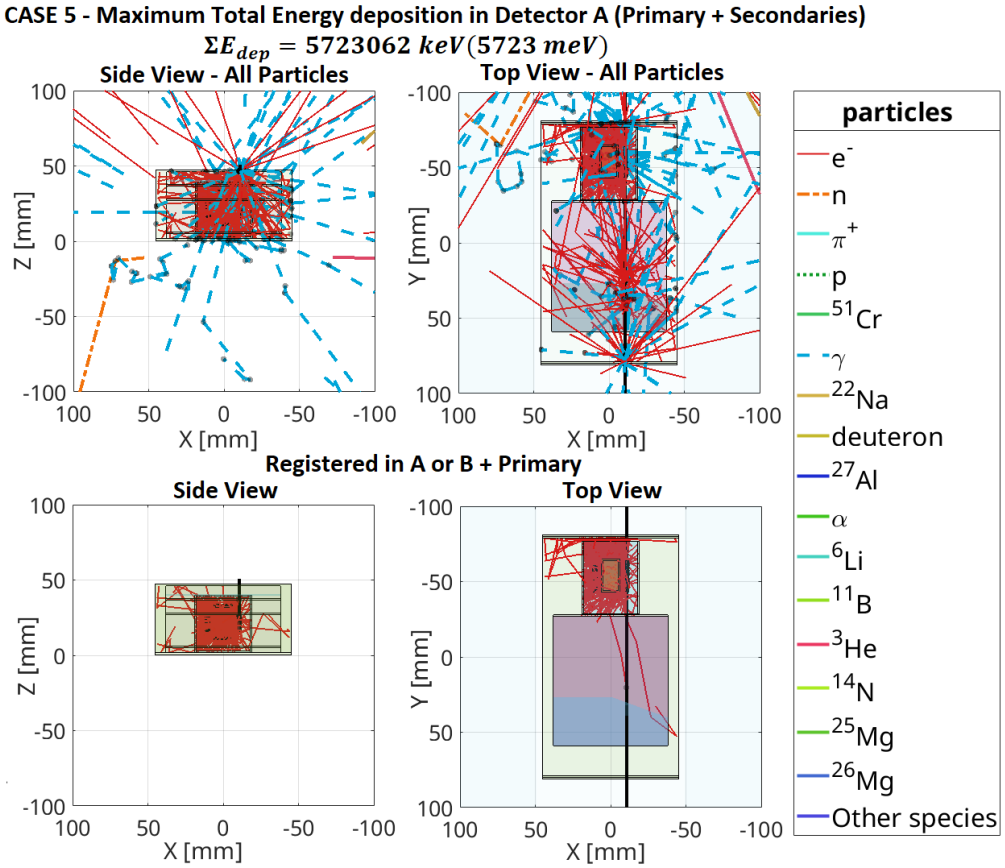


Fig. 5. Case 5 MAX: full and detector-contributing trajectories. Primary Fe-56 traverses the full width of detector A, generating an unusually long path in silicon.

Fig. 5 illustrates the opposite geometrical extreme within Case 5. The primary Fe-56 nucleus travels along the full width of detector A, producing a much longer path in silicon than a conventional 300 µm traversal. The event contains 459,409 tracks and 987,321 steps, with a maximum generation of nine. Detector A receives 5,723.062 MeV, comprising 3,618.920 MeV from the primary Fe-56 track, 2,104.135 MeV from electrons, and approximately 0.006 MeV from photons. Detector B receives 9.760 MeV from secondary electrons, while the primary does not traverse that detector.

The unusually high detector-A signal is thus associated with the extended primary path in the active silicon and the accompanying electron cascade, not with an ordinary traversal through 300 μm of silicon. The minimum and maximum Case 5 events together illustrate how geometry and secondary production can produce widely differing signals within the same event class. A quantitative explanation of the 3.62 GeV primary-track contribution would require step-resolved examination of the primary energy-loss and interaction processes along the full path.

3.4. Quantitative comparison

Table 1. Particle-resolved deposited energy in the two sensitive detectors for all six events (MeV)

Case	Selection	Detector	Fe-56	Fe-55	e−	γ	Total (MeV)
2	MIN	A	0.000000	0.000000	0.070008	0.000000	0.070008
2	MIN	B	0.000000	0.000000	0.926918	0.000000	0.926918
2	MAX	A	0.000000	295.689253	173.588877	0.000313	469.278443
2	MAX	B	0.000000	0.000000	1.370180	0.000000	1.370180
3	MIN	A	50.810296	0.000000	27.898208	0.000000	78.708504
3	MIN	B	51.251112	0.000000	28.326483	0.000029	79.577624
3	MAX	A	73.526768	0.000000	43.695093	0.000208	117.222069
3	MAX	B	73.553916	0.000000	40.992193	0.000000	114.546109
5	MIN	A	7.291630	0.000000	3.872690	0.000049	11.164369
5	MIN	B	0.000000	0.000000	0.789049	0.000000	0.789049
5	MAX	A	3618.920464	0.000000	2104.135136	0.006236	5723.061836
5	MAX	B	0.000000	0.000000	9.759631	0.000000	9.759631

The event selection refers to minimum or maximum deposited energy in detector A, not to cascade multiplicity.

4. Conclusions

Complete Geant4 particle-history reconstruction distinguishes three physically different mechanisms of two-detector coincidence for 1 GeV/nucleon Fe-56 primaries. First, Case 2 demonstrates that secondaries alone can activate both detectors, through electron cascades or heavy nuclear fragments. Second, Case 3 confirms direct primary traversal of both detectors, with additional secondary-electron energy deposition. Third, Case 5 shows mixed registration, in which the primary crosses only detector A while electrons produce the coincidence signal in detector B. The Case 5 extremes further demonstrate the importance of primary path length in silicon: partial traversal near an edge can produce an intermediate signal, whereas traversal along the detector width can lead to exceptionally large energy deposition. The results support event-by-event cascade analysis as a complement to population-level telescope response simulations.

References:

1. Krastev, K. (2026). Numerical Analysis of Genuine and Secondary-Induced Events in the Liulin-MO Telescope aboard ExoMars Trace Gas Orbiter. In: Book of Proceedings, Eighteenth Workshop on Solar Influences on the Magnetosphere, Ionosphere and Atmosphere, pp. 271–281. ISSN 2367-7570. https://doi.org/10.31401/WS.2026.proc